Available online at www.sciencedirect.com
SCIENCE DIRECT®
Journal of Power Sources 123 (2003) 116–125
JOURNAL OF POWER SOURCES
www.elsevier.com/locate/jpowsour

CO tolerance electrocatalyst of PtRu-H_xMeO_3/C (Me = W, Mo) made by composite support method

Z. Hou, B. Yi*, H. Yu, Z. Lin, H. Zhang

Fuel Cell R&D Center, Dalian Institute of Chemical Physics, Chinese Academy of Sciences, Zhongshan Road 457, Dalian 116023, China

Received 27 August 2002; received in revised form 27 March 2003; accepted 31 March 2003

Abstract

CO tolerance electrocatalyst of PtRu-H_xMeO_3/C is prepared by a composite support method, which overcomes evident shortcomings of other preparing methods. According to the result of XRD and TEM, the catalyst shows high dispersion and the H_xMeO_3 exists in amorphous form. The electrooxidations of CO on the catalysts have been investigated in cyclic voltammetry, in which PtRu-H_xMeO_3/C shows lower CO ignition potential according to hydrogen and CO spill over effects, and the bifunctional mechanism is proved to be strengthened for the involvement of H_xMeO_3. The CO tolerances of catalysts are compared according to the PEMFC single cell performance and anode polarization curves operated with H_2/50 ppm CO and H_2/100 ppm CO.

Keywords: Proton exchange membrane fuel cell; CO tolerance; Electrocatalyst; Composite support; TEM; XRD

1. Introduction

Proton exchange membrane fuel cells (PEMFCs) for their characteristics of high-energy efficiency and low emissions are the most promising candidates for electric power generator in transportation applications. Although PEMFCs consuming pure hydrogen can deliver high power densities, it is necessary to use reforming gas instead of pure hydrogen as fuel considering safety and availability issues. Unfortunately, reforming gas typically contains up to 2% CO, which severely poison the Pt anode catalysts, i.e. even a few parts per million of CO produce a substantial degradation in PEMFC performance due to severe anode polarization brought by CO adsorption on electrocatalysts [1,2].

Several strategies have been proposed to overcome CO polarization phenomena in anode compartment of PEMFCs, including the injection of low levels of oxygen or oxygen-evolving compounds in anode fuel flow [3–6], advanced purification of reforming gas according to fuel processor [7], and the development of CO tolerant electrocatalysts [8] and electrode structure [9]. However, oxygen injection method brings about safety issues and lower utilization of fuels. Advanced purification method causes more complexity and cost to the whole systems. Therefore, the most common method approach to solve CO problem is to develop CO tolerant electrocatalysts, which is also the premise of CO tolerant electrode structure.

There was densely researching work on CO tolerant electrocatalyts in the past several decades of years, including binary, ternary even quaternary catalysts. Most of the binary catalysts, alloys usually, e.g. PtRu [10–13], PtSn [14], PtOs [15], PtW [16], PtMo [17,18], show higher activity to CO's electrooxidation reaction (COOR) than Pt does due to bifunctional mechanism, i.e. the second components as Ru, Sn, Os are apt to combine with active water, thus forming oxide as $Ru(OH)_x$, SnO_x and $Os(OH)_x$ which can react with adsorbed CO on platinum, and COOR potential is thus lowered. Many exploring works on ternary and quaternary CO tolerant electrocatalsyts were carried out in recent years [19–23], especially on the system of PtRu-MeO_x (Me = W, Mo, V etc.) [24–30]. Since Tseung and co-workers had found that Pt/WO_3 or PtRu-WO_3 showed higher catalytic activity toward COOR than Pt attributing to hydrogen spill-over effect [24–27], i.e. electrooxidation to hydrogen (HOR) can be spilled over to tungsten oxide when active sites on Pt are blocked by CO, there were some tentative works on the electrocatalysts of Pt or PtRu involving transitional metal oxide.

To meet the application of PEMFC electrocatalyst PtRu-MeO_3 should be prepared regarding such points: (I) as thought commonly PtRu/MeO_x functions as CO tolerant catalysts according to combination of the bifunctional

* Corresponding author.
E-mail address: blyi@dicp.ac.cn (B. Yi).

0378-7753/$ – see front matter © 2003 Elsevier Science B.V. All rights reserved.
doi:10.1016/S0378-7753(03)00515-9

mechanism and hydrogen spill-over effect, the interface between PtRu and transitional oxide should be try to enlarged so as to provide enough active sites for the effect combination; (II) to be the anode catalyst of PEMFC the particle size should be as little as possible so as to provide dense active sites in anode catalytic layer at definite catalyst loading; (III) the preparing condition had better be easily controlled so that the course is well reproductive. Several methods of preparing PtRu-MeO_x or PtRu-MeO_x/C were developed, including freeze-drying method [27], modified Bönnemann method [28], and modified Adams method [29,30]. The electrocatalysts prepared by aforementioned methods show better activities to COOR than PtRu, confirming PtRu-MeO_x to be the promising candidate for the CO tolerant catalysts of PEMFCs. However, the above methods are of some limitations and thus not meet the requirements of applications in PEMFC very well. Both the freeze-drying method and the modified Adams method prepare catalysts of PtRu-MeO_3 through some high temperature courses (300–500 °C), which lead to growing tendency of the noble metal crystal, and thus influencing the dispersion and uniformity of the catalysts. While the preparing condition of modified Bönnemann method must be controlled strictly, and the course is relatively time consuming.

Here, the new preparation of PtRu-H_xMeO_3/C (Me = Mo, W) by a composite support method has been developed. All the preparing course is operated below 100 °C avoiding any effect of high temperature course. The particle size of the catalysts can be controlled at about 2–3 nm with some ordinary conditions. PtRu particle is highly dispersed on a composite support composed of colloidal H_xMeO_3 (Me = W or Mo) and Vulcan XC-72 active carbon, confirmed by X-ray diffraction (XRD) and transmission electron microscopy (TEM). PtRu and transitional metal oxide are well combined and the interface between them is adequately enlarged to promise the combination of bifunctional mechanism and spill over effect, confirmed by the results of electrochemical measurements. It can be observed from cyclic voltammetry (CV) that the COOR potential commences at more negative potential on the catalyst than on PtRu/C. Performance of the PEMFC with the catalysts being the anode catalysts are also presented, which shows better CO tolerance of PtRu-H_xMeO_3/C than PtRu/C.

2. Experimental

2.1. Preparation and characterization of catalyst

PtRu-H_xMeO_3/C was prepared by composite support method following these steps:

1. Sodium tungstate or ammonium molybdate solution was mixed with Vulcan XC72 active carbon to some ratio, and the mixture was stirred vividly.
2. Chloride acid was then added to form H_xMeO_3 colloid, and they were stirred adequately to promise the colloid was adsorbed on the carbon.
3. The mixture was washed by deionized water and dried to form the composite support.
4. Appropriate amounts of H_2PtCl_6 solution and $RuCl_3$ solution were coprecipitated on the composite support, which was dispersed in a mixed solvent of water and isopropyl alcohol.
5. The noble metals were reduced by formaldehyde under alkalescent medium at 80 °C with nitrogen blowing over the reaction. The catalyst was then washed and dried.

PtRu/C was prepared following the steps 4 and 5, and Vulcan XC-72 active carbon was used as support instead of the H_xMeO_3/Carbon composite supports. The content of noble metals in all the catalysts are 20 wt.% Pt and 10 wt.% Ru, and the content of H_xMeO_3 in PtRu-H_xMeO_3/C was 20 wt.%, which was selected after series experiments.

X-ray diffraction measurement was carried out in a Rigaku D/max_2400 system (Cu $K\alpha_1$/40 kV/100 mA), and the angular resolution was 0.02°. Transmission electron microscopy measurements were carried out in a JEOL JEM-2000EX system.

2.2. Electrochemical measurement

The thin film electrode used as work electrode in CV was manufactured as follows: 5 mg catalysts was dispersed ultrasonically in a mixed solution of 1 ml ethanol and 50 μl Nafion solution (5 wt.%). Twenty-five microliters sample was dropped on a glassy carbon substrate to form the electrode, followed with drying at 60 °C to vaporize the ethanol.

The CVs for the catalysts were carried out in Potentiostat of EG&G Princeton Applied Research Model 366A. A conventional three-electrode cell was used in the experiment. Pt foil and a saturated calomel electrode (SCE) were used as counter electrode and reference electrode respectively. All potentials in this experiment are quoted against SCE, which is 0.2412 V versus normal hydrogen electrode at 25 °C. In the measurement pure nitrogen was firstly bubbled in the cell to remove oxygen in the electrolyte solution, the CV was performed till a reproductive curve was acquired. Pure CO was then bubbled in with the potential of work electrode holding at −0.200 V versus SCE, which went on for 30 min to ensure CO saturated adsorption on catalysts. Then, the potential scan was carried out for two circles with scan rate of 20 mV s^{-1} under temperature of 25 °C.

Traditional gas diffusion electrode was applied for both anode and cathode of PEMFC. Membrane electrode assemblies (MEAs) were fabricated by hot-pressing gas diffusion electrodes on Nafion 112 membrane electrolyte. The catalysts loadings were 0.3 mg cm^{-2} Pt for anode and 0.5 mg cm^{-2} Pt for cathode (homemade Pt/C) respectively. The performance of PEMFC single cell with active area of 5 cm^2 was measured on a homemade test station with mass

flow, temperature, and pressure control, and a variable load for recording current-voltage curves. Each test was carried out following such procedures: each MEA was activated with pure hydrogen under 500 mA cm^{-2} until steady performance was acquired; the performance fueled by pure hydrogen was recorded; the fuel was then switched to H_2/CO with current density keeping at 500 mA cm^{-2}; the performance fueled by H_2/CO was then recorded when cell voltage stopped attenuating and held at a steady voltage.

3. Results and Discussion

3.1. XRD patterns for catalysts

It can be seen in Fig. 1 that XRD patterns of PtRu-H_xMeO_3 is similar to that of PtRu/C, and all the catalyst diffractions exhibit only the characteristic diffraction peaks of the face centered cubic phase of Pt bulk, indicating that Pt and Ru had come into being alloy, while the transitional metal oxides existed in amorphous form. The peak broadening caused by little particle size is serious, according to which we can estimate particle size of the catalysts by Scherrer formula [13], i.e.

$$L = \frac{0.9\lambda_{k\alpha 1}}{B_{2\theta}\cos\theta_{\max}} \quad (1)$$

where L is average particle size, $\lambda_{k\alpha 1}$ the X-ray wavelength (1.54056 Å), $B_{2\theta}$ the width of diffraction peak at half-height, and $\theta_{\max}$ the angle at the position of the peak maximum. Diffraction of (2 2 0) peak is fitted to Gaussian on a linear background, and the calculated average particle size according to Eq. (1) is listed in Table 1.

Table 1
Average particle size of the catalysts

	L_{XRD}[a] (nm)	L_{TEM}[b] (nm)	Specific area[c] ($m^2\ g^{-1}$)
PtRu/C	1.8	2.1	133
PtRu-H_xWO_3/C	1.8	2.1	133
PtRu-H_xMoO_3/C	1.9	2.4	117

[a] Average particle size calculated from XRD results according to Eq. (1).
[b] Average particle size estimated statistically from TEM micrographs.
[c] Specific area of catalysts estimated according to Eq. (2).

3.2. Particle size and specific area of catalysts

From the TEM micrographs in Fig. 2, it can be seen that noble metal particle is generally dispersed on the support uniformly, and all the catalysts have similar particle size and morphology. Histograms of particle size distributions for the catalysts are showed in Fig. 3, which include analyses of several regions of the micrograph for each catalyst. The average particle size is estimated statistically from the micrograph as listed in Table 1. According to the micrographs noble metals of both PtRu/C and PtRu-H_xMeO_3/C are highly dispersed uniformly on the supports, and no evident difference is found when the composite support is used instead of carbon support. Although there is some conglomerating effect for catalysts, it should be caused by the catalyst preparing method and not by the influence of composite support. When assuming noble metal in the catalysts exists

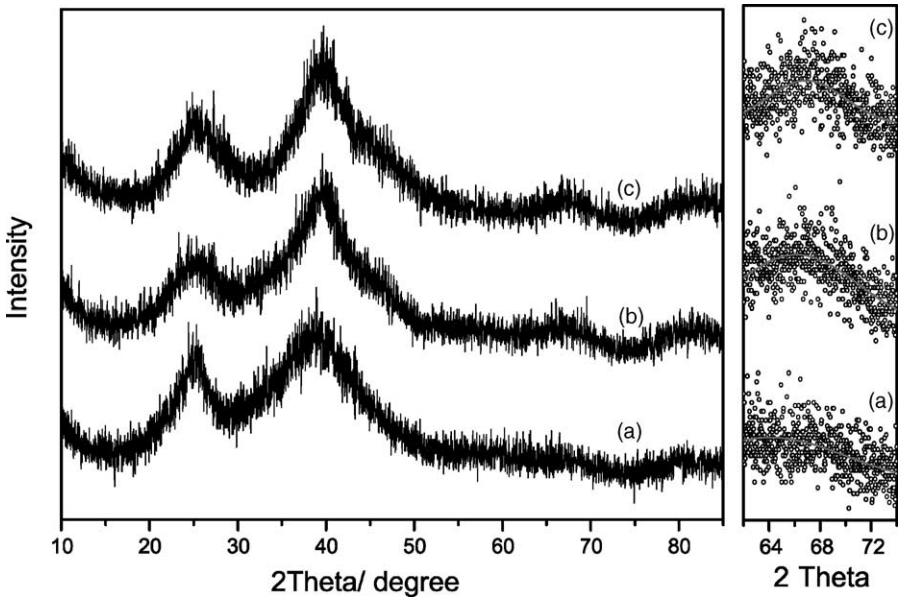

Fig. 1. X-ray diffraction patterns for (a) PtRu/C, (b) PtRu-H_xWO_3/C, (c) PtRu-H_xMoO_3/C. Diffraction peaks in the wide-angle 2θ-scan are indicated in the left figure, and the detailed scan about the (2 2 0) fcc reflection are in the right figure: (○) raw data; (—) least-squares fit to a Gaussian with linear background.

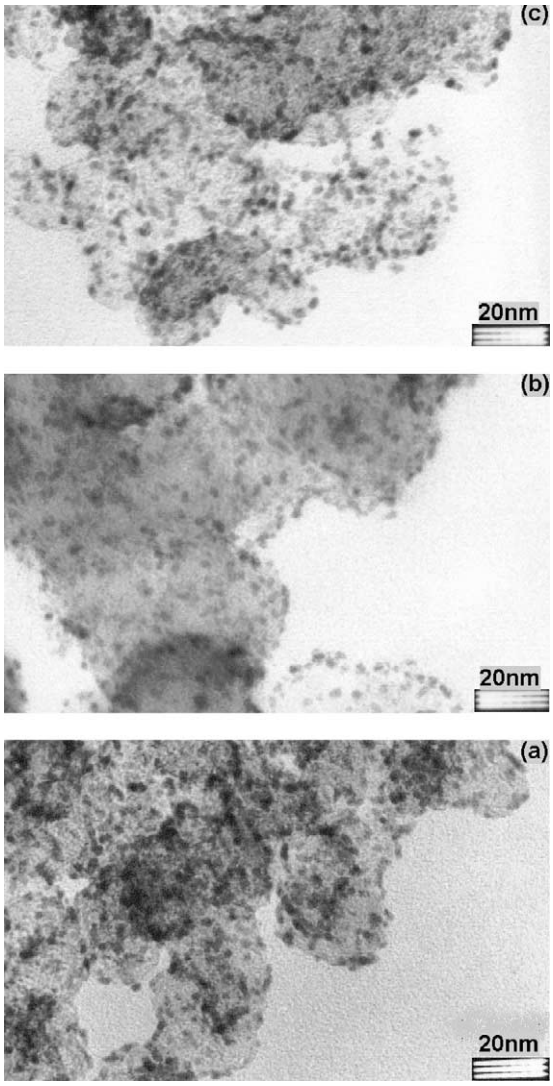

Fig. 2. TEM micrographs for (a) PtRu/C, (b) PtRu-H_xWO_3/C, (c) PtRu-H_xMoO_3/C.

in spherical and homogeneously sized particle, the specific area (S ($m^2\ g^{-1}$)) of the catalysts can be estimated according to the following relation.

$$S = \frac{6 \times 10^3}{\Phi \rho_{Pt}} \quad (2)$$

where Φ (nm) is the average particle size from TEM, ρ_{Pt} ($g\ cm^{-3}$) the platinum density [31]. The results are listed in Table 1.

For HOR is kinetically fast, larger specific area of anode catalyst means more active sites in catalyst [32]. It is thirsty for preparing anode catalyst of PEMFCs with high dispersion or little particle size and good uniformity. From the results of XRD and TEM the transitional metal oxides in the composite support are amorphous, and the particle size of noble metal supported on the composite support is of nanometer range. So when transitional metal oxide is added in active carbon to form the composite support, the deposition process of noble metals is almost unaffected, which means the activity of the catalyst would not be bated.

3.3. CVs in 0.5M H_2SO_4 with CO adsorption

The CVs for the catalysts of CO saturated adsorption are showed in Figs. 4 and 5. COOR occurs in the first anode cycle as showed in Fig. 4, and HOR is depressed thoroughly in the first anode scan due to CO's inhibition of active sites. HOR presents in the second one after vacation of active sites on the catalysts as showed in Fig. 5. It can be seen that both HOR and COOR between PtRu/C and PtRu-H_xMeO_3/C are of remarkable difference according to the shape of the peaks.

3.3.1. HOR in the second anode scan circle

In Fig. 5, contrasting to PtRu/C new peaks at 0.05 V for PtRu-H_xWO_3/C as indicated by arrow I and 0.2 V for PtRu-H_xMoO_3/C as indicated by arrow II are overlapped with the peak of HOR on PtRu at nearly −0.16 V. It was the hydrogen spill over effect caused by the noble metals and the transitional metal oxide in the composite support that brings the new HOR peaks as showed by expression (3), in which Me = W and Mo:

$$MeO_3 + xPt - H \rightarrow HxMeO_3 + xe + xPt \rightarrow MeO_3 + xe + xH^+ + xPt \quad (3)$$

Although it is hard to calculate active area of PtRu-H_x MeO_3/C according to the integrating area of HOR peak in CV for the overlapping of peaks, it can be affirmed that the active area of noble metals in PtRu-H_xMeO_3/C is close to that of PtRu/C according to the intensity of HOR peak at −0.16 V. Therefore, total activity to hydrogen of PtRu-H_xMeO_3/C should be better than PtRu/C when the catalytic oxidation of hydrogen through hydrogen spill over effect on PtRu-H_xMeO_3/C is considered.

3.3.2. COOR in the first anode scan circle

As showed in Fig. 4 the COOR on PtRu/C commences at about 0.2 V, and there is almost no current happens at potential below the COOR oxidation potential. While the current commences at −0.15 V on PtRu-H_xMeO_3/C, lower nearly 0.35V than that on PtRu/C. The current of COOR on PtRu-H_xMeO_3/C can be divided into two parts from the CVs in Fig. 5, i.e. the current caused by hydrogen spill over effect (I_H) at potential below 0.2 V and the current of COOR (I_{CO}) beyond 0.2 V, which can be identified more clearly in CV of PtRu-H_xWO_3/C.

Compared with I_H in Fig. 5, that I_H of CO adsorption in Fig. 4 does not decrease indicates that HOR via hydrogen spill over way occurs immunized from CO poisoning. As indicated in Eq. (3), Pt active site is needed during the hydrogen spill over effect reaction course, while at the potential

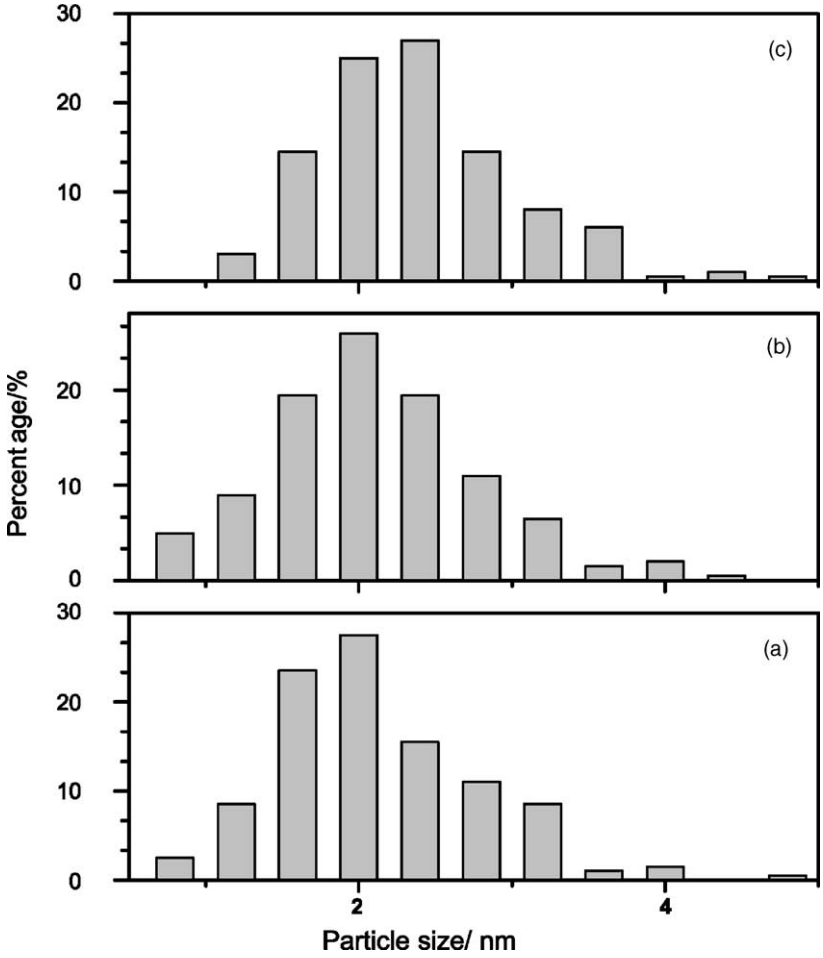

Fig. 3. Particle size distributions estimated from TEM micrographs for (a) PtRu/C, (b) PtRu-H_xWO_3/C, (c) PtRu-H_xMoO_3/C.

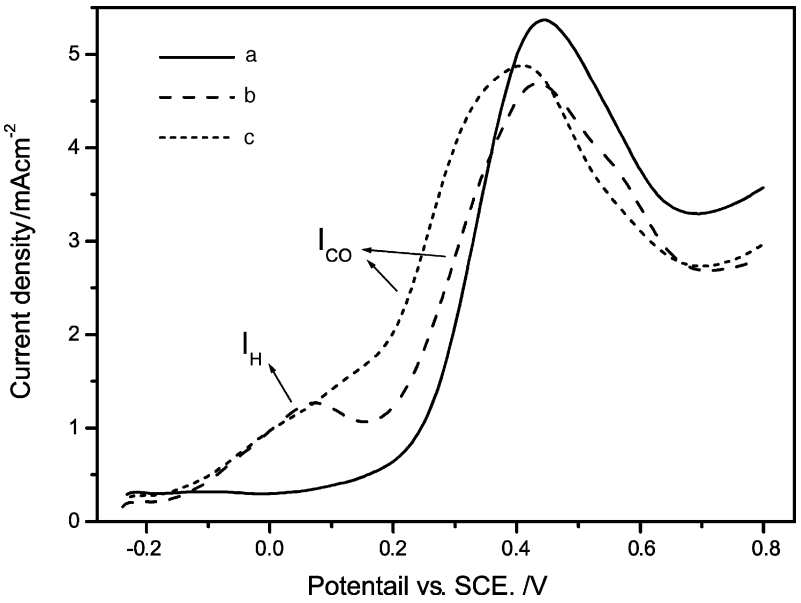

Fig. 4. The first anode scan in cyclic voltammograms for CO oxidation on (a) PtRu/C, (b) PtRu-H_xWO_3/C, and (c) PtRu-H_xMoO_3/C in 0.5 M H_2SO_4 solutions at room temperature (25 °C) with scan rate of 20 mV s^{-1}.

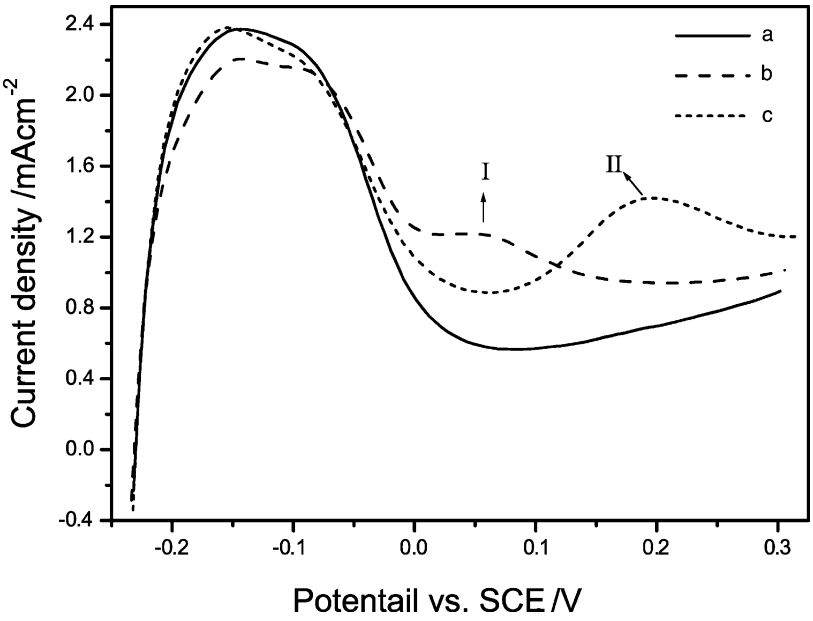

Fig. 5. The second anode scan in cyclic voltammograms for hydrogen oxidation on (a) PtRu/C, (b) PtRu-H_xWO_3/C, and (c) PtRu-H_xMoO_3/C in 0.5 M H_2SO_4 solutions at room temperature (25 °C) with scan rate of 20 mV s^{-1}.

below 0.2 V the active sites is almost inhibited by CO thoroughly. Therefore, it may be concluded that CO adsorption on noble metals in PtRu-H_xMeO_3/C is weakened due to effect of the composite support, and more active sites could be offered at potential below 0.2 V in CV of PtRu-H_xMeO_3/C than that of PtRu/C.

It is evident that I_{CO} commences at lower potential on PtRu-H_xMeO_3/C than on PtRu/C, indicating that the COOR reaction mechanism has varied due to the interaction between noble metals and the composite support. COOR at low potential runs through such a way as indicated in expression (4), which is likely to HOR on PtRu-H_xMeO_3/C and therefore can be regarded as CO spill over
effect.

$$\begin{array}{l} CO + OH \longrightarrow CO_2 + H^+ + e \\ \quad | \quad\quad | \\ Pt- \quad MeO_3 \end{array} \qquad (4)$$

On the other hand, H_xWO_3 exists in an amorphous form that can be expressed as $MeO_3{\cdot}xH_2O$. Such waters bonded to MeO_3 weakly are easier to be decomposed under the catalysis of Ru than waters in electrolyte. Therefore, $Ru(OH)_x$ can be formed at more negative potential on PtRu-H_xMeO_3/C than on PtRu/C, i.e. the bifunctional mechanism on PtRu can be strengthened by the involvement of $MeO_3{\cdot}xH_2O$. So COOR according to bifunctional mechanism, as showed in expression (5), on PtRu-H_xMeO_3/C runs at more negative potential than on PtRu/C.

$$M - CO + Ru - OH \rightarrow CO_2 + H^+ + e; \quad (M = Pt, Ru) \qquad (5)$$

The most important criterion for estimating CO tolerance of electrocatalysts is the ignition potential, at which CO adsorbed on the catalyst is oxidized and the current rises rapidly [33]. According to the results of CVs the ignition potential PtRu-H_xMeO_3/C is lowered to −0.15 V, more negative about 350 mV than that of PtRu/C, which is due to the spill over effect and more effective bifunctional mechanism for the involvement of H_xMeO_x. Therefore, measured by this criterion the CO tolerance of PtRu-H_xMeO_3/C is much better than PtRu/C. The catalysts prepared by the composite support method are thus believed to acquire enough interface between noble metals and transitional metal oxide to give a well combined function.

3.4. PEMFCs' single cell performances with hydrogen contaminated by CO

Single cell performances operated with pure hydrogen, H_2/50 ppm CO and H_2/100 ppm CO are showed in Fig. 6. All the cells give similar performances when pure hydrogen is used, showing that the dispersion of three catalysts is resembled, as confirmed by TEM and XRD. It can be found that the performance of PtRu-H_xWO_3/C electrode is a little higher than other two, because that the hydrogen spill over effect increases effectively active area of the catalyst. Although there is also evident hydrogen spill over effect on PtRu-H_xMoO_3/C, the over potential for the spill over reaction, as showed in Fig. 5, counteracts its contributions to the increase of the active area. When using H_2/CO as fuel, cell performances of PtRu-H_xMeO_3/C electrode are better than that of PtRu/C, indicating that the combination of CO

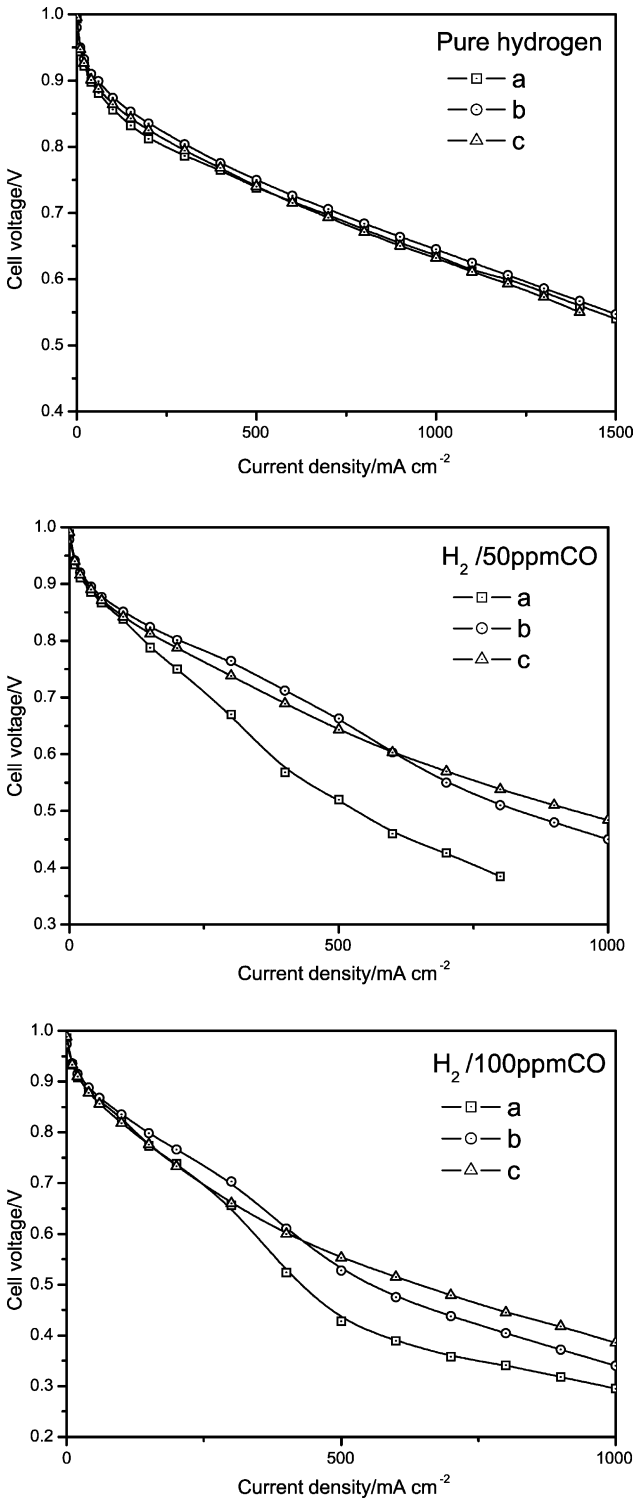

Fig. 6. PEMFCs' single cell performances of (a) PtRu/C, (b) PtRu-H_xWO_3/C, and (c) PtRu-H_xMoO_3/C anode: 80 °C of cell temperature, 80 °C for both humidifiers, 0.2 MPa of operating pressure.

spill over effect and the forenamed strengthened bifunctional mechanism in PtRu-H_xMeO_3/C enhances their CO tolerance. More details about CO tolerance of the catalysts in the PEMFCs are discussed as below.

To analyze the anode polarization by CO in PEMFC, the anode polarization curves for three catalyst electrodes are deduced as follows. Overall cell voltage can be expressed by Eq. (6):

$$V = V_0 - \eta_a - \eta_c - iR \tag{6}$$

where V_0 is the open-circuit potential, i the current density, η_a and η_c the anode and cathode overpotentials respectively, R the cell resistance including membrane resistance and interfacial resistance. Therefore, the difference in the polarization of the anode between the cases of the presence ($\eta_{H_2/CO}$) and the absence of CO (η_{H_2}) in the anode feed can be obtained by making measurements of the cell voltage under otherwise identical experimental conditions, as showed in Eq. (7):

$$\eta_{H_2/CO} - \eta_{H_2} = V_{H_2} - V_{H_2/CO} \tag{7}$$

Since the overpotential for pure hydrogen can be neglected without substantial error, the anode overpotential difference can be simply expressed in Eq. (8). In fact such simplification might bring about 50 mV error when the current density increases to 1 A cm^{-2}, however, the influence exists in all the three electrodes, so the comparison is tenable.

$$\eta_{H_2/CO} \approx V_{H_2} - V_{H_2/CO} \tag{8}$$

The anode polarization curves according to Eq. (8) for catalysts operated with H_2/CO are showed in Fig. 7. The polarizations below 100 mA cm^{-2} are so slight that can be neglected, for there are enough active sites for HOR in the catalyst layer to provide such a low current density. Three catalysts are characteristic of different slope region in their polarization curves, which represent their CO tolerance.

According to Tafel equation as indicated in Eq. (9),

$$\eta = a + b \lg i \tag{9}$$

hydrogen over potential is linear with the current density i. The first linear region in the polarization curve at low current density belongs to Tafel region, in which the over potential is mainly caused by HOR. When the current density increase to the value that there is not enough active sites in the catalytic layer to keep the current because of CO poison, the over potential begins to increase steeply forming the second linear region. When the over potential increases to the COOR potential, CO is electrooxidized and the polarization reverts to hydrogen over potential forming the third linear region which is also a Tafel region. The linear regions of polarization curve for the three catalyst electrodes operated with H_2/50 ppm CO and H_2/100 ppm CO are listed in Table 2, including the current density district and the slope of each linear region.

Because the third linear region can be evidently observed only in the polarization curve of PtRu/C electrode in case of H_2/100 ppm CO, they are not listed in Table 2. The wider i range of the first linear region and the smaller slope of the second linear region mean the less anode polarization caused by CO poison. According to Table 2, the first

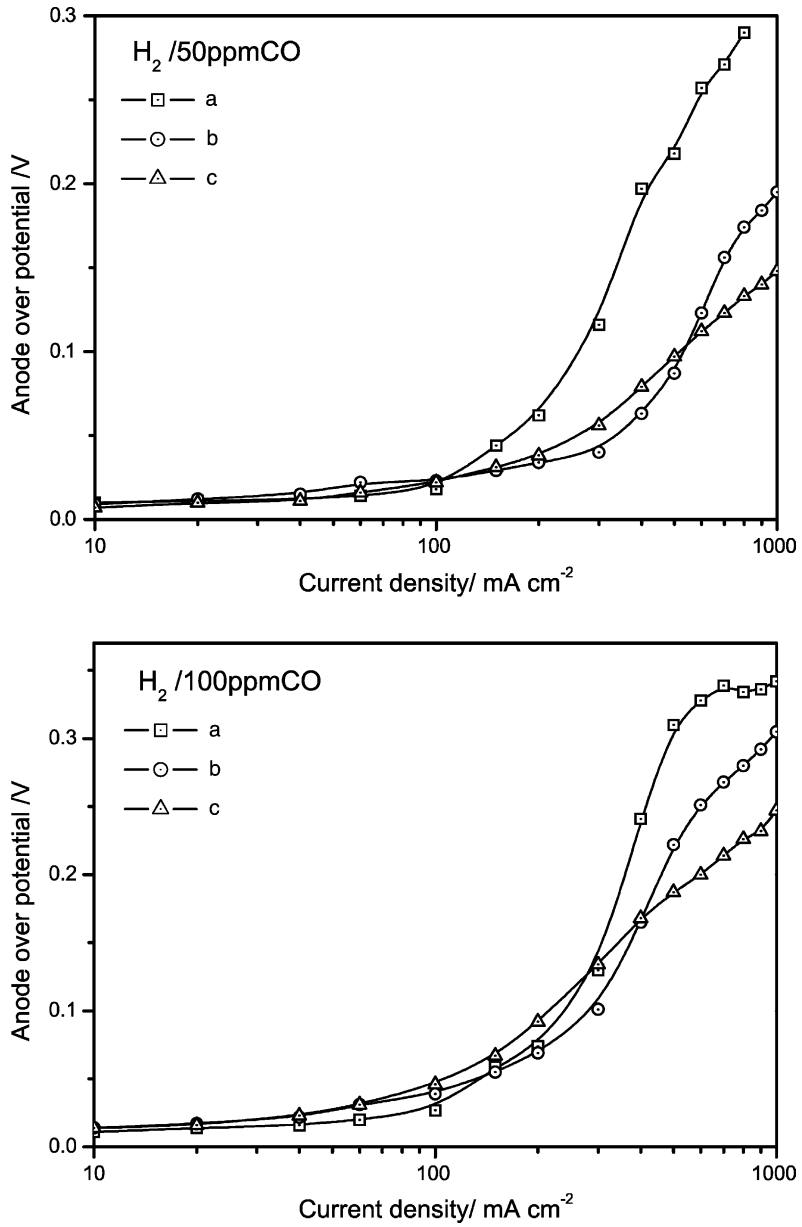

Fig. 7. PEMFCs' anode polarization curves of (a) PtRu/C, (b) PtRu-H_xWO_3/C, and (c) PtRu-H_xMoO_3/C anode: 80 °C of cell temperature, 80 °C for both humidifiers, 0.2 MPa of operating pressure.

Table 2
The different linear regions in the polarization curves

		First linear region		Second linear region	
		i range[a] (mA cm^{-2})	Slope[b] (V dec^{-1})	*i* range[a] (mA cm^{-2})	Slope[b] (V dec^{-1})
PtRu/C	H_2/50 ppm CO	10–100	0.00737	100–800	0.3283
Electrode	H_2/100 ppm CO	10–100	0.01485	100–500	0.3981
PtRu-H_xWO_3/C	H_2/50 ppm CO	10–300	0.02073	300–1000	0.3224
Electrode	H_2/100 ppm CO	10–100	0.02501	100–1000	0.3018
PtRu-H_xMoO_3/C	H_2/50 ppm CO	10–200	0.02288	200–1000	0.1645
Electrode	H_2/100 ppm CO	10–100	0.03073	100–1000	0.2087

[a] The current density range for the linear region in Fig. 7.
[b] The slope of the linear region in Fig. 7.

linear region extends to 300, 200 and 100 mA cm^{-2} for PtRu-H_xWO_3/C, PtRu-H_xMoO_3/C and PtRu/C in case of H_2/50 ppm CO respectively, indicating that the spill over effect on PtRu-H_xMeO_3/C provides additional current so that the polarization caused by CO is delayed to higher current density compared to PtRu/C. However, when the CO content increased to 100 ppm, the range difference of the first linear region lessens. In the second linear region in which CO poison polarization functions, the slope of the curves is sorted as PtRu-H_xMoO_3/C < PtRu-H_xWO_3/C < PtRu/C for both H_2/50 ppm CO and H_2/100 ppm CO, which is accordant to the ignition potential sort of the catalysts, further confirming that the strengthened bifunctional mechanism on PtRu-H_xMeO_3/C enhances their CO tolerance.

The Tafel slopes of the two linear regions in Table 2 represent the reaction mechanism for the electro-oxidation. In the first linear region, i.e. the hydrogen electro-oxidation region, the PtRu-H_xMeO_3/C electrodes show similar slope values, different from the value of PtRu/C electrode, confirming that they electro-catalyze hydrogen oxidation through the same mechanism, in which the hydrogen spill over effect are included. Although the slopes of PtRu-H_xMeO_3/C electrodes are a little higher than that of PtRu/C electrode, they extend the hydrogen electro-oxidation region to higher current density, especially for the PtRu-H_xWO_3/C electrode, which should be more beneficial to improve the cell performance under CO contaminated fuel. In the CO electro-oxidation linear region, the slopes of PtRu-H_xMeO_3/C electrodes are

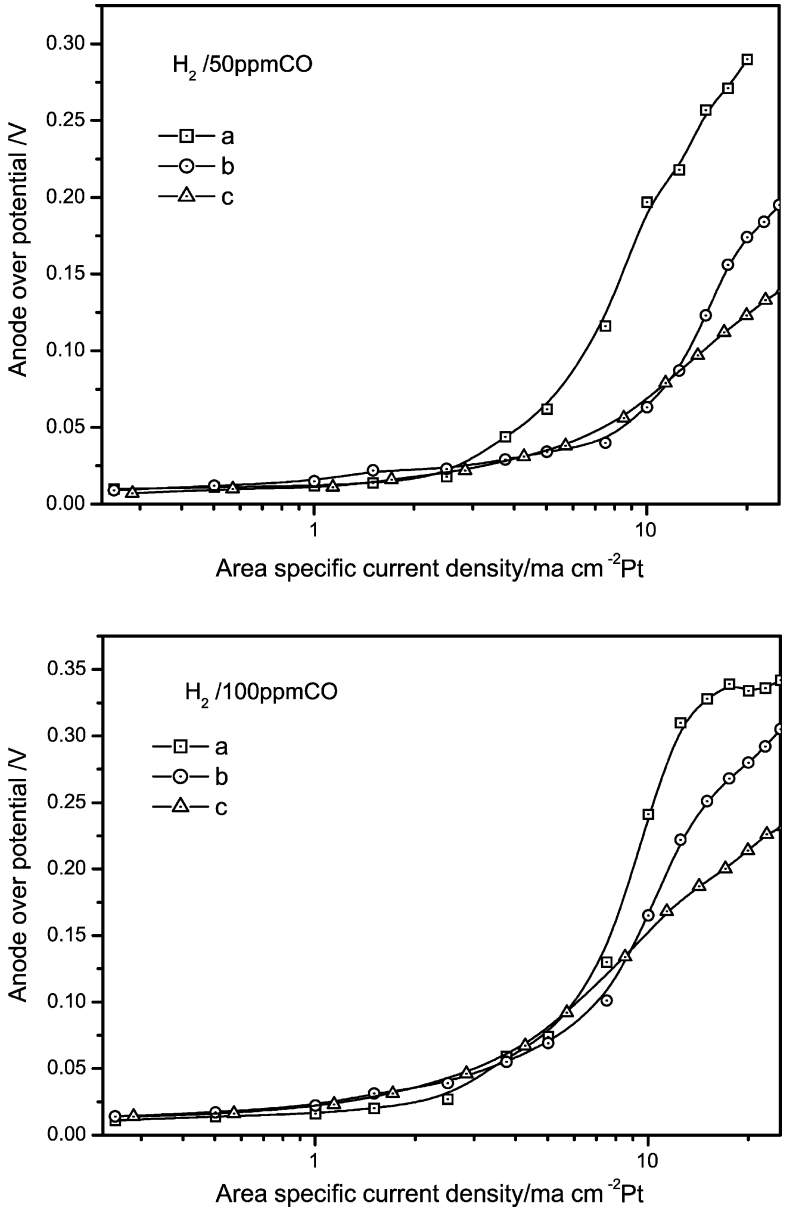

Fig. 8. PEMFCs' anode polarization curves normalized by the electrode surface area of (a) PtRu/C, (b) PtRu-H_xWO_3/C, and (c) PtRu-H_xMoO_3/C anode: 80 °C of cell temperature, 80 °C for both humidifiers, 0.2 MPa of operating pressure.

lower than that of PtRu/C electrode. However, they are not as close as in the hydrogen electro-oxidation region, especially in case of H_2/50 ppm CO, indicating the slight difference between the two catalysts in CO electro-oxidation course. It is speculated that they obey the same mechanism, i.e. the combination of CO spill over effect and strengthened bifunctional mechanism as discussed in Section 3.3.2. However, PtRu-H_xMoO_3/C shows more effective combination by its lower slope than PtRu-H_xWO_3/C does. Generally, PtRu-H_xMeO_3/C improves the CO tolerance, but PtRu-H_xWO_3/C depends more on hydrogen spill over effect and extends the hydrogen Tafel region current density range, while PtRu-H_xMoO_3/C depends more on improving CO electro-oxidation ability by more effective CO spill over effect, which is also confirmed by the CV results in Figs. 4 and 5.

Since the catalyst loading for the three electrodes are same, the polarizing curves in Fig. 7 are in fact vs the mass specific current density, which is important measure for the catalytic activity from a practical point of view. While the polarizing curves vs the area specific current density, which is normalized to the surface area of the electrodes, can reflect the effects of catalyst structures such as particle sizes and chemical state. Since the structures of three electrodes are consistent, the active surface area of the electrodes should depend on the specific area of the catalysts. Therefore, we give the comparison of over-potential to the area specific current density in Fig. 8, which is normalized to the *S* in Table 1. It can be seen that they are very close to the curves in Fig. 7 because three catalysts are of little difference in their dispersions. The same conclusion with former discussion according to Fig. 7 can be drawn.

4. Conclusion

The dispersions of noble metals in PtRu-H_xMeO_3/C prepared by composite support method are not affected by the addition of transitional metal oxide, i.e. H_xWO_3 and H_xMoO_3, which exist in amorphous form. Furthermore, composite method can provide enough interfaces between noble metals and transitional oxides in the catalysts. Such a structure promises better CO tolerance than PtRu/C for lowering the ignition potential to COOR and improving the HOR current when active sites on noble metals blocked by CO. Hydrogen and CO spill over effect are believed to occur on transitional metal oxides, which leads to delay of CO poison polarization in PEMFC anode. The bifunctional mechanism of COOR is strengthened for the existence of active water bonded on the transitional metal oxides, and the anode polarization caused by CO poison is so diminished. The composite support method is therefore promising for preparing the CO tolerance catalyst.

References

[1] H.-F. Oetjen, V.M. Schmidt, U. Stimming, F. Tuilla, J. Electrochem. Soc. 143 (1996) 3838–3842.
[2] H. Yu, Z. Hou, B. Yi, Electrochemistry (China) 7 (2001) 238–243.
[3] S. Gottesfeld, US Patent 4910099 (1990).
[4] S. Gottesfeld, J. Pafford, J. Electrochem. Soc. 135 (1998) 2651–2652.
[5] V.M. Schmidt, H.-F. Oetjen, J. Divisek, J. Electrochem. Soc. 144 (1997) L237–L238.
[6] R.J. Bellows, E. Marucchi-Soos, R.P. Reynolds, Electrochem. Solid-State Lett. 1 (1998) 69–70.
[7] T.V. Choudhary, D.W. Goodman, Catal. Lett. 59 (1999) 93–94.
[8] Z. Hou, H. Yu, B. Yi, M. Han, Electrochemistry (China) 6 (2000) 379–387.
[9] H. Yu, Z. Hou, B. Yi, Z. Lin, J. Power Sources 105 (2002) 52–57.
[10] U.A. Paulus, U. Endruschat, G.J. Feldmeyer, T.J. Schmidt, H. Bönnemann, R.J. Behm, J. Catal. 195 (2000) 383–393.
[11] T.J. Schmidt, M. Noeske, H.A. Gasterger, R.J. Behm, Langmuir 13 (1997) 2591–2595.
[12] M. Watanabe, N. Uchida, S. Motoo, J. Electroanal. Chem. 229 (1987) 395–406.
[13] V. Radmilovoc, H.A. Gasteiger, P.N. Ross Jr., J. Catal. 154 (1995) 98–106.
[14] E.M. Crabb, M. Robert, T. David, J. Electrochem. Soc. 147 (2000) 4440–4447.
[15] Y. Zhu, C.R. Cabrera, Electrochem. Solid-State Lett. 4 (2001) A45–A48.
[16] E. Passalacqua, F. Lufrano, G. Squadrito, A. Patti, L. Giorgi, J. New Mat. Electrochem. Syst. 3 (2000) 131–135.
[17] P. Gouérec, M.C. Denis, D. Guay, J.P. Dodelet, R. Schulz, J. Electrochem. Soc. 147 (2000) 3989–3996.
[18] B.N. Grgur, N.M. Markovic, P.N. Ross, J. Electrochem. Soc. 147 (2000) 1613–1619.
[19] A.S. Aricò, P. Cretì, N. Giordano, V. Antonucci, J. Appl. Electrochem. 26 (1996) 959–967.
[20] M. Götz, H. Wendt, Electrochim. Acta 43 (1998) 3637–3644.
[21] A. Lima, C. Coutanceau, J.-M. Léger, C. Lamy, J. Appl. Electrochem. 31 (2001) 379–386.
[22] M. Goetz, H. Wendt, J. Appl. Electrochem. 31 (2001) 811–817.
[23] R. Liu, H. Iddir, Q. Fan, G. Hou, A. Bo, K.L. Ley, E.S. Smotkin, J. Phys. Chem. B 104 (2000) 3518–3531.
[24] A.C.C. Tseung, K.Y. Chen, Catal. Today 38 (1997) 439–443.
[25] P.K. Shen, K.Y. Chen, A.C.C. Tseung, J. Electrochem. Soc. 142 (1995) L85–L86.
[26] K.Y. Chen, P.K. Shen, A.C.C. Tseung, J. Electrochem. Soc. 142 (1995) L185–L187.
[27] K.Y. Chen, Z. Sun, A.C.C. Tseung, Electrochem. Solid-State Lett. 3 (2000) 10–12.
[28] C. Roth, M. Goetz, H. Fuess, J. Appl. Electrochem. 31 (2001) 793–798.
[29] K. Lasch, L. Jörissen, J. Garche, J. Power Sources 84 (1999) 225–230.
[30] Z. Jusys, T.J. Schmidt, L. Dubau, K. Lasch, L. Jörissen, J. Garche, R.J. Behm, J. Power Sourecs 105 (2002) 297–304.
[31] B. Le Gratiet, H. Remita, G. Picq, J. Catal. 164 (1996) 36–43.
[32] B. Yi, H. Yu, Z. Hou, Z. Lin, J. Zhang, P. Min, H. Zhang, Precious Met. (China) 23 (2003) 1–7.
[33] B.N. Grgur, N.M. Markovic, P.N. Ross, Electrochim. Acta 43 (1998) 3631–3635.